

## Contents

<b>A1. Factual information .....</b>	<b>2</b>
<b>A1.19 Useful or effective investigation techniques .....</b>	<b>2</b>
A1.19.1 Use of data memories from mobile phones and cameras .....	2
A1.19.2 Evaluation of the sound characteristics of the engines.....	5
A1.19.3 Methodology for the reconstruction of HB-HOT flights .....	9
A1.19.4 Methodology for photogrammetric evaluations.....	11
A1.19.5 Methodology for numerical analysis.....	12
A1.19.6 Background information for the flight path analysis.....	13

**A1. Factual information**

**A1.19 Useful or effective investigation techniques**

A1.19.1 Use of data memories from mobile phones and cameras

The Ju 52/3m g4e was not equipped with any accident-resistant recording devices such as a flight data recorder (FDR) or a cockpit voice recorder (CVR), as is common and mandatory in commercial air transport aircraft today. FDRs specifically log flight parameters such as altitude, speeds, accelerations, heading, attitudes and positions. CVRs register conversations and radio communications as well as other sounds in the cockpit on various channels.

These days, the majority of light aircraft and gliders are also fitted with a basic recording device, such as a Flarm<sup>1</sup> collision warning device or a GPS logger.

As the historic Ju 52 aeroplane attracted attention during its flight, a good number of pictures and video recordings showing HB-HOT from the outside were available for the investigation. Several appeals were made to the public, which generated images and video footage of HB-HOT providing great support for the investigation. The images and videos capturing the outside of the aircraft supplemented the existing material and the descriptions of eyewitnesses in the vicinity of the accident site.

From inside the aircraft, primarily the recording devices belonging to the passengers, such as analogue or digital cameras and mobile phones as well as their electronic memory chips or SD cards<sup>2</sup> were of interest. The majority of this evidence was severely damaged and contaminated.

Using the STSB's own resources and with the help of Forensic Services from the cantonal police of Grisons, it was possible to recover some of the data from these storage units. The data from severely damaged components were recovered by the French safety investigation authority – the *Bureau d'Enquêtes et d'Analyses pour la Sécurité de l'Aviation Civile* (BEA) – and other specialist laboratories.

Out of the 44 electronic devices secured, the data from ten data storage units could be read.

A1.19.1.1 Preparations for data recovery

The electronic components were taken apart, cleaned and their data storage units removed in an ESD<sup>3</sup>-protected area in the BEA laboratory in Paris (see figure 1). For certain mobile phones, in addition to the data storage unit, the associated encryption unit had to be removed as well, so that the data could also be read at a later stage. After cleaning, the data storage units were dried in a special oven for approximately 72 hours.

---

<sup>1</sup> A Flarm is a collision warning device with the additional capability of logging altitudes and positions of the flight. GPS loggers can do the same with regards to the flight path.

<sup>2</sup> An SD card, meaning a secure digital memory card, is an electronic data storage device.

<sup>3</sup> ESD: Electrostatic discharge can damage electronic components.

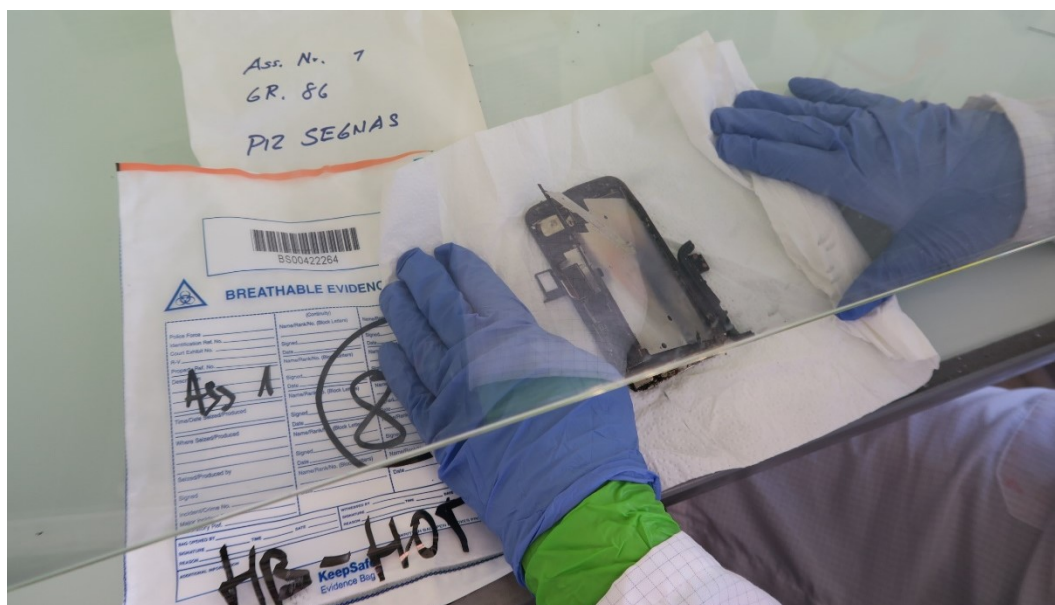


**Figure 1:** Removal of the data storage unit from a damaged mobile phone in the BEA laboratory.

For the mobile phones, data was recovered using the Golden Chassis method. For this, identical mobile phones to the ones secured from the aircraft were procured and their data storage and encryption cards were removed. Subsequently, the exhibits' processed data storage and encryption units were installed in the new Golden Chassis devices. For some of the devices, this restored access to the data and allowed it to be read.

In the cases where the data could not be retrieved after the data storage units had been rebuilt, internal defects were suspected in their data storage cards. Using a special CT<sup>4</sup> device available at the BEA, which heavily magnified the observed objects, it was possible to examine the inside of the data storage cards and chips without damaging them and to detect any defects.

Some of the mobile phones exhibited cracks in the very small quartz components on their data storage card and could not be read. However, the data storage blocks in the main data storage unit and in the encryption unit were intact.

Using nano soldering technology, the data storage chips and the encryption unit were removed and reinserted on an identical and intact Golden Chassis data storage card. The Golden Chassis data storage card was then inserted into the Golden Chassis phone.

Some of the mobile phones were damaged to such an extent that the silicon blocks in the data storage units were broken or destroyed. In these cases, it was not possible to repair the data storage units.

SD cards that could not be repaired using IT forensics were also analysed using a CT device. Their internal circuitry and the silicon blocks in the data storage units were assessed for damage (see figure 2).

<sup>4</sup> CT: Computed tomography is an imaging procedure used in radiology. Objects are X-rayed so that they can then be viewed three-dimensionally on a computer.

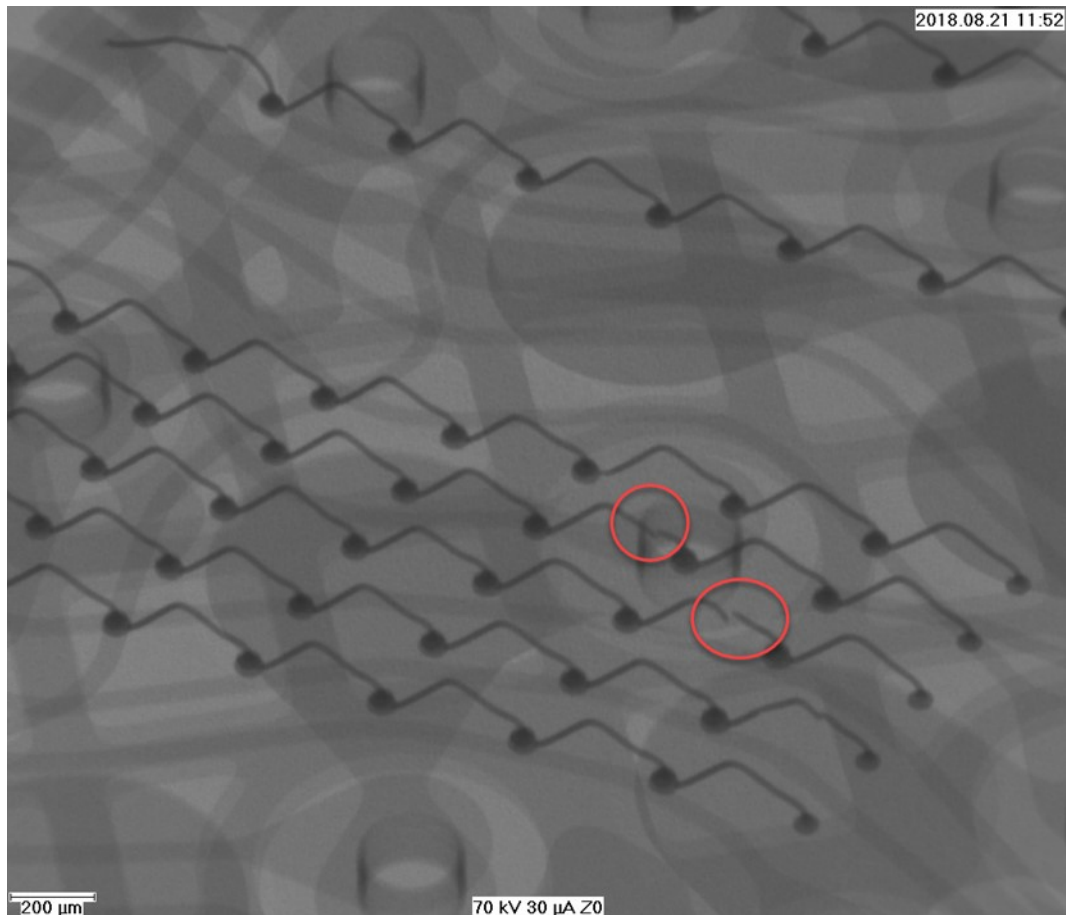


**Figure 2:** Heavily magnified CT scan of an SD card. Damage to the circuitry within is circled in red. Source: BEA.

#### A1.19.1.2 Data recovery and reading of the data

The data storage units of each device were read and assessed with regards to the data's relevance concerning the HB-HOT flights on 3 and 4 August 2018. Individual images and video footage could be restored in this process.

A passenger's GoPro camera contained a defective and incomplete video file. This was recorded during the accident and could not be completely written to the SD card due to the damage caused to the device as a result of the impact. Using BEA methods, it was possible to restore this video file in high resolution (4K). In addition, it was possible to read the buffering cache<sup>5</sup> of the camera in order to obtain additional lower-resolution video material. This allowed for an additional 5.06 seconds of video and audio material to be restored.

The lower-resolution footage is congruent, frame by frame, with the 4K footage and is 5.06 seconds longer, as mentioned above. Following recovery, this longer, lower-quality footage exhibited image interference and loss of images at two locations, totalling 2.17 seconds. It was, however, possible to replace the missing individual frames of the video footage with frames from the high-quality footage as, at that time in the video, the two streams were running in parallel and featuring identical images. Only the lower-quality video exhibited desynchronisation between the video and the corresponding sound, starting from the location of the image interference. The audio tracks of the two videos were binarily identical over their entire

---

<sup>5</sup> A camera's cache buffers the frames taken before compressing and writing them to the SD card as an MP4 video file.

common runtime and were therefore not subject to a failure in recording. Thus, the chronological sequence of the images and sound could be reconstructed despite some missing images.

#### A1.19.1.3 Data evaluation of image and video data

Further data evaluation was based on the recovery of the data on the damaged data storage units from the recording devices belonging to the aircraft passengers. Individual images and videos were analysed. The audio track was removed from some of the video footage and sonographically evaluated using spectral analysis. Details on this method and the procedure can be found under section A1.19.2.

The reconstructed photographs of the entire trip on 3 and 4 August 2018 were assigned to the respective flight paths. In many instances, the time stamps in the image files did not match the actual time as they were dependent on the date and time set in the recording devices. Nevertheless, it was not a problem to reconcile the relative time between two images with the flight path. For each reconstructed unit, a separate relative timeline was set up. By using the subjects captured in the images, it was possible to confirm the respective aircraft position. The method applied is explained in greater detail under section A1.19.3.

The recovered videos were also assigned to the flight path and thus to a common timeline. Individual videos could be recovered which were recorded in the cockpit of HB-HOT during the flights on 3 and 4 August 2018. Using the audio tracks of the footage made it possible to determine the rotational speeds of the propellers and the engines, and to compare them with the displays in the cockpit from the video images. The video footage taken closer to the time of the accident was analysed in greater detail. The video files were additionally split into their individual frames. A selection of these individual frames was photogrammetrically analysed. Details on this procedure can be found under section A1.19.4.

#### A1.19.2 Evaluation of the sound characteristics of the engines

As no flight recorder data was available, there was no information on the number of engine revolutions. In order to obtain this data, the audio tracks of video footage were used. Larger moving parts such as propellers, pistons, gears and crankshafts generate typical acoustic signals that can be evaluated using spectral analysis to create sonograms. A sonogram represents the different frequencies of sound over time. Stronger signals are depicted more intensively or are more intense in colour. Subsequently, the frequencies and the individual components' rotational speeds derived from those frequencies can be determined for the respective video footage. Furthermore, attention was paid to changes in the sound signature, looking out for unfamiliar or unexpected noises in the sonogram that could be suggestive of a technical defect in the aircraft.

It was possible to evaluate the videos' audio files containing characteristic sound signatures of Ju-Air's Ju 52 aeroplanes. These analyses were carried out by specialists in the BEA laboratory. The audio tracks of 23 video files of HB-HOT, from inside the aircraft and on the ground, as well as of a sister aircraft were examined. Detailed sonograms were produced for ten audio tracks. The Doppler effect<sup>6</sup> was taken into account for recordings that were taken from outside the aircraft. In addition, video footage available online was used to determine the standard sound spectrum for other Ju 52 aeroplanes.

---

<sup>6</sup> When the source of a sound and an observer move relative to one another, the received frequency will differ from the sent frequency depending on the relative speed between the source and the observer. The Doppler effect has to be taken into account in the sonographic evaluation.

Generally, it was possible to identify each engine's crankshaft rate (CSR), blade rate (BR) of the propellers, and cylinder rate (CR) for all of their nine cylinders. As can be seen in figure 3, the most distinct noises were emitted by the propellers. As the aircraft featured directly driven fixed-pitch propellers, it was possible to determine the identical speed of the propeller and its corresponding engine at known times of the video recordings.

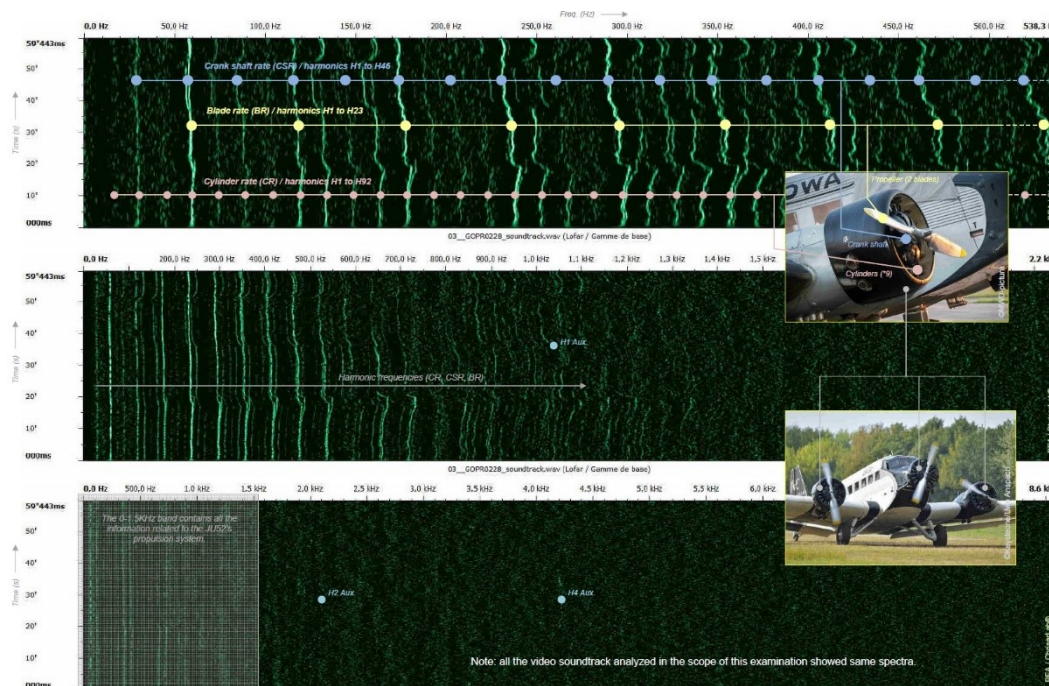


**Figure 3:** Example of a sonogram for a video recording from the cockpit of HB-HOT. The identified components CSR (blue), CR (pale red) and BR (yellow) are labelled. The images of the aircraft show the components. Here, the y-axis describes the time and the three x-axes describe the frequencies in three different amplifications. The harmonic frequencies of the main signal caused by interferences are also visible. Source: BEA.

When sonographically analysing video recordings that have been filmed from the cabin of an aircraft, a high level of accuracy with regard to engine speeds can be assumed, varying by just a few hertz (Hz).

For the engine speeds calculated from all of the sonograms analysed, the engines were assigned as engine A, B and C for each video sequence. It was, however, not possible to assign the determined speeds to the actual engines.

#### A1.19.2.1 Engine synchronisation

During the video recording relating to figure 3 as well as some other video footage, passengers were videoing the outside from the cockpit. When doing so, the engine instruments could be seen in the footage.

In the cockpit, the engine speed (rpm) is displayed on three tachometers featuring analogue and digital gauges. The digital gauge in the middle shows the speed of the centre engine. The digital gauges for the left and right engines each show the difference in speed for the respective engine in relation to the centre engine. In figure 4, the digital gauge for the centre engine shows a speed of 1,727 rpm. The left engine tachometer displays a value of + 3 (1,730 rpm); the right engine tachometer displays a value of + 2 (1,729 rpm).

When all three engines run at slightly different speeds, it is not uncommon for acoustic standing waves to be formed. These unpleasant interferences are perceived as low-frequency, rising and falling ambient noise. By synchronising the left and right engines as best as possible, the centre engine can be operated at a higher or lower speed. This allows fine adjustments to be made without interferences occurring.

The digital gauges are used to synchronise the engines as closely as possible; adjustments can be made by slightly moving the throttle levers. Due to lack of accuracy, fine adjustment for synchronisation of two engines is not possible using an analogue gauge. It must be made by observing the digital gauges. This means that at least one of the pilots' pairs of eyes will linger on these gauges for a longer period of time.



**Figure 4:** Tachometers with digital displays, marked by yellow rectangles. The yellow arrows point to the three throttle levers that must be operated to set the respective rpm.

#### A1.19.2.2 Advanced technical sonogram analysis

##### A1.19.2.2.1 General

The BEA was able to determine the engine speeds in individual phases of the two flights from Dübendorf to Locarno on 3 August 2018 and the accident flight from Locarno on 4 August 2018 using the ten sonogram analyses carried out overall.

In the following section, the fly-by past Mount Rigi is shown as an example.

The video sequence shows in-cockpit footage on which the main aircraft instruments are visible. Thus, using still images, it is possible to identify the analogue read-outs for the engine speeds as well as the indicated altitude and airspeed. In some still images documenting the flight past Mount Rigi, the digital engine-speed gauges could also be seen. The BEA recorded the speeds determined from the pictures and compared these with the speeds determined through analyses.

For most of the sonographically evaluated flights flown by the accident crew, it stood out that the propellers were synchronised very delicately, slowly and precisely. The engines were regularly resynchronised. In this sense, a flight crew leaves a 'fingerprint' on the sonogram when handling the engines.

#### A1.19.2.2.2 Mount Rigi fly-by

Figure 5 shows a graph of the three engine speeds from HB-HOT during its flight past Mount Rigi on 3 August 2018. The yellow, red and green dots indicate the rpm speeds of the three engines read from the analogue gauges in the still images over the course of the fly-by. In some still images, it was also possible to see the digital displays of the tachometers. These are shown as numbers in the square brackets relate to the speed of the centre engine, the numbers to the left and right of these brackets correspond to the speed differences of the left and right engine in relation to the centre engine.

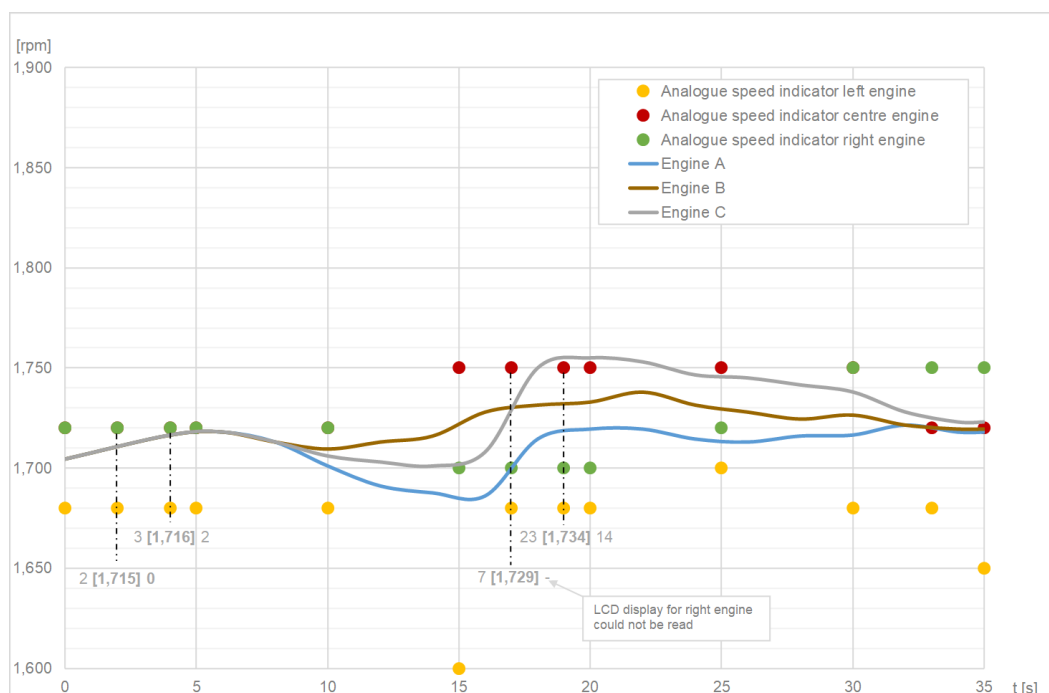


**Figure 5:** Graph of the engine speeds from HB-HOT over the course of the video footage recorded whilst flying past Mount Rigi on 3 August 2018.

In the first phase of the fly-by, the engine speeds were between 1,700 and 1,720 rpm. After 15 seconds, the speeds of engines A and C were increased by 20 to 30 rpm, now ranging between 1,720 and 1,750 rpm. The speed of engine A never exceeded 1,720 rpm.

The graph reveals that there are considerable discrepancies between the speeds determined from sonogram analysis and those read from the still images displayed in analogue form on the gauges. At 20 seconds, for example, the speed from the sonogram ranges between 1,720 and 1,750 rpm, whilst the values read from the analogue gauges range from 1,680 to 1,750 rpm.

At the 2-, 4-, 17- and 19-second marks in the video footage, it was also possible to read the three digital tachometers from the respective still images. This established that the four readings corresponded rather accurately to the respective sonogram analysis speeds.

The fly-by was performed at an indicated altitude ranging between 1,805 and 1,810 m AMSL. The indicated airspeed was in the range of 150 to 165 km/h.



**A1.19.2.3 Conclusion of the BEA report on its sonographic evaluation**

The BEA report and further investigation came to the conclusion that the same sound signatures that are characteristic and typical for Ju 52 aeroplanes can be ascertained in all the sonograms evaluated, be it from the accident aircraft or from audio tracks of another Ju 52/3m g4e. Furthermore, with regards to all recordings including accident video footage from inside the aircraft as well as impact videos from outside the aircraft, the following can be stated:

- No unusual or unfamiliar noises were apparent on any of the recordings.
- The analysis did not reveal any spectral anomaly concerning HB-HOT's propulsion system, neither for the engines nor the propellers. Near the Segnespass, there were no anomalies or faults in the propulsion system either.
- The analysis allowed for the engine speeds set for HB-HOT during each flight phase (take-off, climb, cruise, accident sequence) to be determined. On the approach to the Segnespass and in most other cases, it was possible to examine the three engine speeds individually.
- Further analysis combined with the results from the examination of the engine instruments revealed great inaccuracies in HB-HOT's analogue tachometers. The digital displays were much more accurate.

**A1.19.3 Methodology for the reconstruction of HB-HOT flights**

The reconstruction of the flight paths was primarily based on radar recordings from multi-radar tracking (MRT), i.e. data compiled from several radar systems at different locations. Due to terrain topography, the flight path positions ascertained from radar data vary in accuracy, particularly for flights in mountainous areas, and can deviate considerably from the actual positions. Several positions in a row may be missing, resulting in gaps in a radar flight path. The flight altitudes relating to the radar positions are transmitted as pressure altitudes based on the ICAO standard atmosphere; they have been corrected with an accuracy of  $\pm 30$  m for the following examinations based on the actual pressure conditions.

In addition, a wide range of images and video footage, as well as statements of numerous eyewitnesses who were watching HB-HOT from the ground, were available for the investigation, as well as image and video material from devices belonging to the passengers found at the scene of the accident.

The images and video footage were visually evaluated in the geometry of the terrain. Based on the evaluation of these data and the information obtained, the gaps in the radar flight paths could be filled in most instances, the inaccuracies eliminated to a large extent, and the flight paths reconstructed (see figure 6).

In order to determine the positions of the aircraft in space, its attitude relative to the terrain and its speed relative to the ground, complex photogrammetric evaluations were carried out, especially for the decisive flight phase before the accident. For this purpose, the basin south-west of Piz Segnas was surveyed using a 3D laser scanner and the measurements were incorporated into the three-dimensional terrain model of the Swiss Federal Office of Topography (Swisstopo). To determine the relevant details of a three-dimensional model for a Ju 52/3m g4e aircraft, a laser scan was taken of one of HB-HOT's sister aircraft. By using a series of specific software programs for the creation and processing of three-dimensional models as well as for image processing, it was possible to determine the positions and attitudes of HB-HOT based on images captured on cameras both inside the aircraft and on the ground.

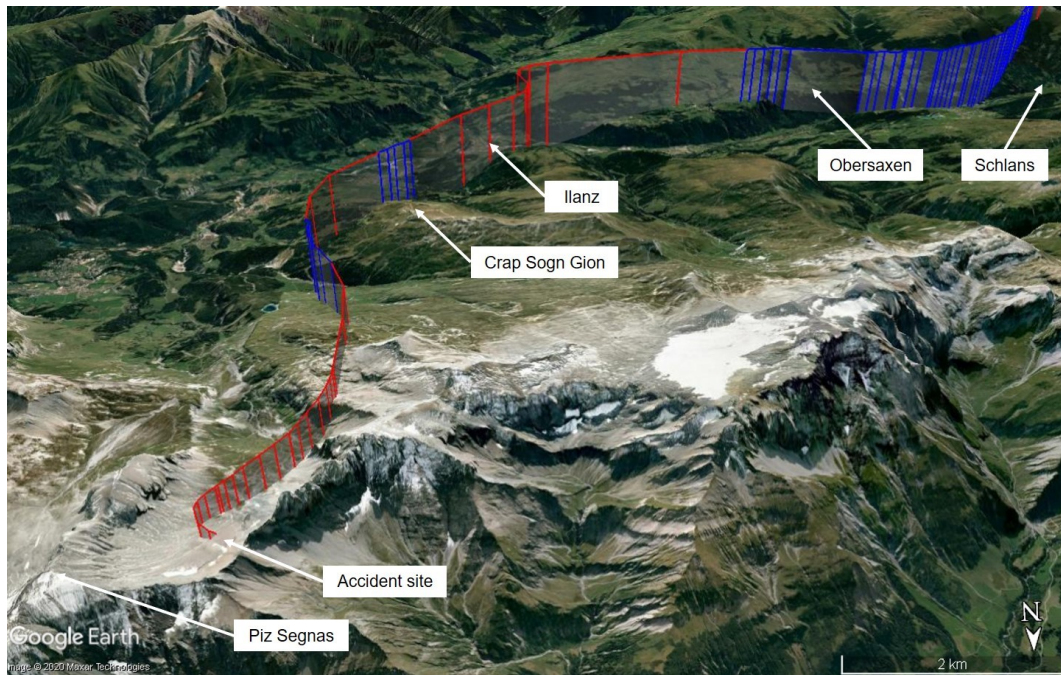


**Figure 6:** Section of the accident flight on 4 August 2018 with stretches derived from radar data (blue) and that have been reconstructed (red). Shown on Google Earth.

The radar data points corrected in height are marked in the sections shown in blue, connecting them to the ground with vertical lines. In addition to position and altitude, MRT also calculates and records the time and ground speed (GS) for each data point. In the absence of radar data points, a missing stretch can be filled in with a straight line between adjacent known positions based on the information available – provided that no alternative flight paths are possible, as was the case near Obersaxen (see figure 6).

Some of the missing or obviously inaccurate radar flight path sections, which could not be connected by a straight line taking into account the above considerations, could be reconstructed based on the observations of eyewitnesses on the ground. Emanating from the positions established by these eyewitnesses, the lines to the sighted aircraft were constructed in three-dimensional space using their descriptions. The aircraft's spatial positions were then determined through iteration, as was the case near Ilanz (see red stretch of flight path in figure 6). To check the plausibility of such a flight path section, the average speed relative to the ground was calculated based on the length of the flight segment and the time difference between the adjacent known data points; this was then compared with the GS of the adjacent data points.

Where pictures of the passing aircraft, taken from the ground, were available, the reconstruction of the flight segments was carried out in the same way as described above, i.e. the images were visually incorporated into three-dimensional terrain models, thereby devising the lines of sight.

In order to determine the positions of the aircraft in space, its attitudes in relation to the terrain and its speed relative to the ground, the much more precise, photogrammetric evaluations mentioned earlier in this section were carried out for the decisive flight phase before the accident in the basin south-west of Piz Segnas (see section A1.19.4).

**A1.19.4 Methodology for photogrammetric evaluations**

The Zurich Forensic Science Institute (FOR) was commissioned with the photogrammetric analysis of images and video footage obtained from eyewitnesses who had watched the Ju-Air aircraft from the ground as well as from passenger devices. In addition to the reconstruction of HB-HOT's accident flight path, especially in the last flight phase before the accident site, individual positions and attitudes of the Ju-Air aircraft were determined in order to objectively assess the risks during flight operations.

The methods used and the results of these photogrammetric evaluations were described in detail by the forensic institute. The following sections briefly summarise key elements of the methodology used.

Individual sections of terrain and objects were surveyed using a 3D laser scanner, both from the ground and from the air using a helicopter. The point clouds produced from this were then combined into a single point cloud using the appropriate software. Subsequently, this point cloud was photogrammetrically evaluated, together with the corresponding image series, and high-resolution 3D models of the photographed objects or sections of terrain were computed.

Two-dimensional photographs and video images from cameras with a distorted perspective were algorithmically restored and then incorporated into the three-dimensional models using reference points and specialised software. These methods, described here in a very simplified manner, allowed for the photogrammetric evaluation of both images captured from known locations (eyewitnesses on the ground) as well as from unknown locations (passengers' images).

The level of accuracy of an aircraft's positions and attitudes in space determined in this way very much depend on the image quality as well as the camera's location and direction of view, among other things. For example, the positions and attitudes can be determined more accurately if they are based on images taken from the aircraft abeam the direction of flight, overlooking a wing against a backdrop featuring distinctive terrain, than those lacking the aforementioned elements. Several iterations – in which the parameters were varied up to pixel blur – were required before it was possible to specify the most appropriate position and attitude of the aircraft.

For these reasons, the level of accuracy with regards to the individual positions and attitudes varies from case to case and cannot be quantified universally. It was possible to determine some positions and attitudes to within a few decimetres and less than 0.1 degree respectively, whilst, with a particularly unfavourable scene captured in the image, the position in the direction of the flight was determined with an accuracy of up to 90 m. This margin of error was taken into account when using the values determined, for example in the reconstruction of the flight paths and the calculation of the ground speeds.

The following model representation exemplifies the result of the photogrammetrically reconstructed positions and flight attitudes of HB-HOT in the last flight phase before the accident.

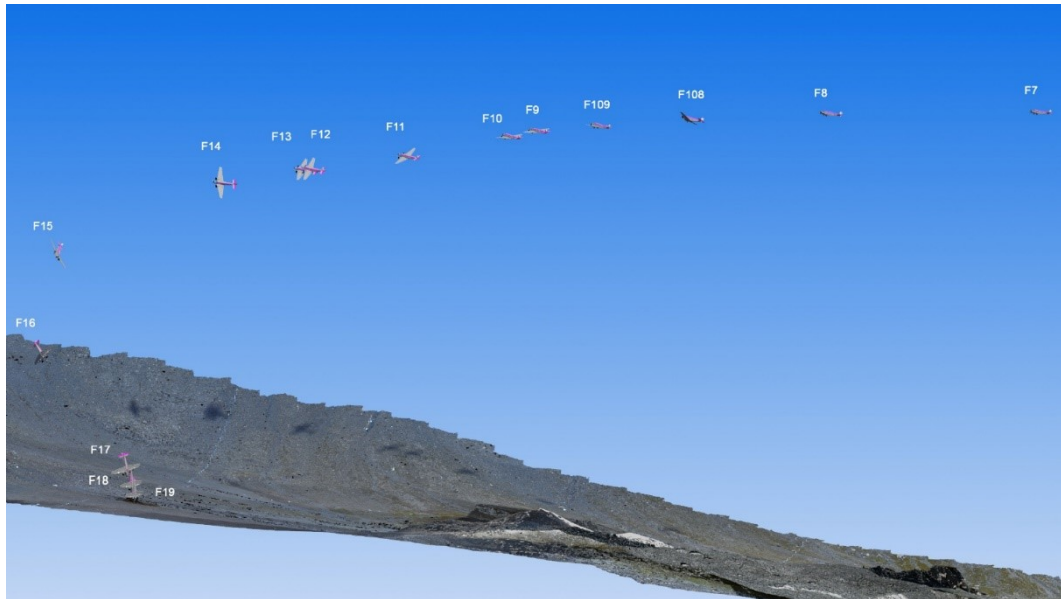


**Figure 7:** Photogrammetrically reconstructed positions and flight attitudes (F7 to F19) of HB-HOT in the last flight phase before the accident, depicted using the scan data of the terrain.

#### A1.19.5 Methodology for numerical analysis

The numerical evaluations are based on data determined through photogrammetry, in particular the positions and attitudes of the aircraft in space. The following pieces of additional data were used to assess the flight phase from the accident flight when the aircraft entered the section of terrain surrounding the Segnespass:

- Results of the meteorological evaluation, in particular the wind speeds and wind directions, based on COSMO analysis (see annex [A1.7](#));
- Results (sonograms) of the evaluation carried out by the BEA of acoustic data from a video recorded from inside the aircraft;
- Results of a visual, qualitative assessment of the aileron deflection carried out by the STSB based on video footage recorded from inside the aircraft.

##### A1.19.5.1 Methodology and precision in the use of radar data

As part of a multi-radar tracking (MRT) system, a data point is recorded every four seconds. The radar data of a 60-minute flight consists of about 1,000 radar data points. The lateral positions are average values from the bearings of all radar stations. Due to terrain topography, these flight path positions ascertained from radar data vary in accuracy, particularly for flights in mountainous areas, and can deviate considerably from the actual positions. After loss of the radar signal in particular, the continued flight path is extrapolated for a few seconds. These and other inaccuracies as well as the system inaccuracies described below were known and taken into account during further investigation.

The accuracy of the lateral radar positions was discussed in collaboration with Skyguide, the operator of the radar system. Under ideal conditions, a lateral error in the range of 30 m can be assumed. When several radar stations cover an area, placed at an ideal angle to each other, an accuracy of 30 to 60 m or better can normally also be achieved in the mountains. With poor radar coverage, the lateral error can be significantly higher. However, the terrain, as well as the altitude flown and the time elapsed between missing radar data points, allow conclusions to be drawn about the possible flight paths.

When the STSB experts assessed the flights based on radar data, they assumed a lateral radar data inaccuracy of a maximum of  $\pm 150$  m.

The altitudes in the radar recordings are pressure altitudes based on the ICAO standard atmosphere transmitted by the aircraft's transponder. This means that a properly calibrated transponder signal can be assigned to the pressure prevailing at flight altitude (QFE). This in turn is known with an accuracy of 0.5 to 1.0 hPa (about 5 to 10 m vertically) due to the pressure field known from station measurements and model calculations (see annex [A1.7](#)). This allowed for the altitudes recorded in increments of 100 ft (about 30 m) to be converted to true altitudes and for them to be compared with the ground level elevation. Inaccuracies relating to both the method and the analysis of flight phases using GPS coverage show an accuracy of  $\pm 15$  m in altitude. Together with a digitalisation inaccuracy relating to the transponder's height increments, an overall inaccuracy of 30 m can be assumed.

#### A1.19.6 Background information for the flight path analysis

Determined, aerodynamically possible turn radii can only be achieved if the necessary kinetic energy is available, be it through the power available from the engines or through the conversion of potential energy into kinetic energy when the aircraft descends in a controlled manner.

In the evaluation of the flights from summer 2018, a total aircraft mass of 9,500 kg was used as a basis for gauging the turn radii. As an aircraft cannot be operated accurately at its stall speed ( $v_s$ ), a safety margin of 30% has been included on  $v_s$  to calculate the turn radii possible at a bank attitude of 30 degrees. This margin is very low for when flying in high-altitude mountains and is equivalent to the margin referred to in the aircraft flight manual (AFM) for the final approach when landing. Turns were assumed for normal passenger flight operation with a bank attitude of a maximum of 30 degrees. Possible turn radii were considered at minimum speed (with the 30% stall margin) and additionally with the actual speed without any wind influence.

The reaction time when approaching a ridge, crest or similar at 90 degrees to the direction of flight was assessed at seven seconds. Five seconds were adopted for the time taken to recognise an unfavourable situation (downdraught, engine failure, other aircraft, etc.) and map out alternatives, and two seconds for initiating any necessary measures such as bank attitude and engine adjustments.

For the section of the flight near the Segnespass, the determined aircraft mass of 9,206 kg was used for the calculation. According to the table in the AFM, the indicated stall speed in this configuration is 107 km/h indicated airspeed (IAS), which corresponds to a true airspeed (TAS) relative to the surrounding air at the density altitude near the Segnespass prevailing at the time of the accident of 125 km/h. The aerodynamically possible radii and figures near the Segnespass were calculated without a safety margin or other allowance.

Turn radii in relation to the terrain were estimated using the ground speed (TAS with the assumption of  $GS = TAS$ ). Aerodynamically possible maximum bank attitudes were calculated using the assumed IAS. Temperature and air pressure were taken into account as density altitude. Additional factors can slightly change the stall speed ( $v_s$ ) at higher altitudes. This was neither taken into account in the AFM, nor in this investigation.

In contrast to TAS, IAS decreases at higher altitudes due to lower air density. A constant IAS at a higher altitude results in significantly greater turn radii due to the increased TAS. This fact was taken into account in the calculations.